



Synthesis and characterization of β -Ag₂Se and β -AgCuSe nanoparticles via facile precipitation route

P. PRATHIBA JEYA HELAN¹, K. MOHANRAJ¹, G. SIVAKUMAR²

1. Department of Physics, Manonmaniam Sundaranar University, Tirunelveli 627 012, India;
2. CISL, Department of Physics, Annamalai University, Annamalainagar, Tamil Nadu-608 002, India

Received 2 August 2014; accepted 10 December 2014

Abstract: β -Ag₂Se and β -AgCuSe nanoparticles were synthesized using AgCl precursor instead of conventional AgNO₃ by simple precipitation method. It was found that orthorhombic structures were obtained for both β -Ag₂Se and β -AgCuSe nanoparticles. The result shows Ag₂S as impurity while increasing the concentration of AgCl. Moreover, the microstructural images show polyhedral and pebble-like particles. The band gap energy is increased for β -Ag₂Se owing to small crystallite size. The AgCl precursor can effectively produce pure nanoparticles. Hence, it is interesting in terms of identification of potential precursor for synthesizing β -Ag₂Se and β -AgCuSe nanoparticles.

Key words: β -Ag₂Se; β -AgCuSe; nanoparticle; AgCl precursor; precipitation method

1 Introduction

Silver selenide nanoparticles have semiconducting as well as metallic properties and exist in different polymorphic phases. The low temperature phase below 400 K was identified as β -Ag₂Se with a structure of orthorhombic and the high temperature α -Ag₂Se has BCC structure [1]. Semiconductor properties are observed at low temperatures and metallic-like conduction is generally believed to occur above the critical temperature [2].

The α -Ag₂Se belongs to the family of super ionic conductors which are of present and future technological interest. It is used as solid electrolyte in photochargeable batteries, multipurpose ion-selective electrodes, infrared sensors, electrochemical storage cells, electrochemical potential memory devices, and magnetic field sensing devices [3,4].

Semiconducting β -Ag₂Se compound is rarely found in the nature as mineral naumannite [3]. β -Ag₂Se is a promising material for technological applications in various fields such as thermo-chromic material for non-linear optical devices, photoconductors, photovoltaic cells, photo sensitizer in photographic films [5–7]. Besides, β -Ag₂Se nanostructures exhibited excellent

photocatalytic activity for the degradation of Rhodamine B under UV light irradiation. Additionally, they display superhydrophobic characteristics [7]. β -Ag₂Se is an important n-type semiconductor with a narrow band gap [3]. The recent studies on optical properties of Ag₂Se have exhibited the optical band gap energy between 1.2 and 1.8 eV [6]. Many researchers have explored the synthesis of Ag₂Se nanoparticles via simplest routes such as sonochemical [8–10], solvothermal [7,11] and solid state reaction [12] methods under mild and nontoxic conditions.

The incorporation of copper metal ions in the semiconducting low temperature Ag₂Se system leads to the formation of super ionic conducting Silver copper selenide (AgCuSe) ternary compound. In recent years, AgCuSe has sporadic attention in the mineralogical literature due to its many interesting physical properties. The Ag–Cu–Se system exhibits mixed conduction mechanisms, i.e., partly electronic and partly ionic conductivity at room temperature [13]. AgCuSe is a superionic conductor with exceptional large ionic conductivity in the superionic phase. Hence, it has more application in electrochemical devices such as batteries, fuel cells and gas sensors [14]. It exists in two phases where the β -AgCuSe phase indexes orthorhombic structure and α -AgCuSe phase indexes cubic

structure [15]. AgCuSe was synthesized by fusing the elements in vacuum, mechanical alloying, solidification, hydrazine reduction at the boiling temperature, and simple redox reaction at room temperature, respectively [13,14,16].

AgNO₃ was widely used as a silver source for the synthesis of Ag-based nanoparticles, while there is not much work found for AgCl as precursor since it is insoluble in water. In many reactions, AgNO₃ combines with chlorine ions to yield AgCl residues. These waste AgCl by-products could be used as an alternative precursor for AgNO₃ in the preparation of Ag₂Se nanoparticles. Hence, it is motivated to synthesize low temperature Ag₂Se and the ternary AgCuSe nanoparticles using AgCl. In this work, we reported the preparation and characterization of β -Ag₂Se and β -AgCuSe nanoparticles using the inorganic precursor AgCl by precipitation method.

2 Experimental

The AR grade chemicals AgCl, SeO₂, Na₂SO₃ and CuSO₄·5H₂O were used. First, 1 mol/L SeO₂ was dissolved in 20 mL distilled water under constant stirring for 30 min. Meanwhile, 0.25 mol/L Na₂SO₃ was dissolved in 15 mL distilled water under constant stirring for 30 min. Then, the two solutions were mixed together and again stirred well for 30 min to obtain a homogeneous solution.

Similarly, 0.5 mol/L AgCl was dissolved in 15 mL NH₃·H₂O, and the solution was stirred for 30 min and it was added into the mixed solution. The composite solution again stirred well for 30 min. Subsequently, a clear black precipitate was obtained. It was filtered by using filter paper and was kept in the oven at 80 °C for 1 h. The dried sample was finely ground by using mortar and pestle. Similar procedure was adopted to synthesize Ag₂Se nanoparticles with 1 mol/L AgCl, 2 mol/L SeO₂ and 1 mol/L Na₂SO₃ solutions.

To prepare AgCuSe, 0.25 mol/L CuSO₄ was dissolved in 10 mL distilled water under constant stirring for 30 min and the rest of the experimental steps were adopted similarly to that of Ag₂Se. The prepared solution was added into the composite solution. Consequently, blue precipitate was obtained. The structural characterization was carried out by analyzing the XRD patterns obtained using Cu K_α radiation ($\lambda=1.5406$ Å) with an X'pert PRO X-ray diffractometer. The presence of vibrational modes of functional groups is identified from the Fourier transform infra red (FTIR) spectral analysis in the range of 4000–400 cm⁻¹ by Perkin Elmer FTIR spectrometer with resolution of ± 4 cm⁻¹. The optical measurements were performed using Hitachi U3400 UV–Vis spectrometer. The surface morphology

was recorded using JEOL SEM model JSM–5610 LV with an accelerating voltage of 20 kV, at high vacuum (HV) mode and secondary electron image (SEI).

3 Results and discussion

3.1 X-ray diffraction analysis

Figure 1(a) shows the XRD pattern of β -Ag₂Se nanoparticles obtained at 0.5 mol/L AgCl, 1 mol/L SeO₂ and 0.25 mol/L Na₂SO₃. It can be seen from the diffraction pattern that the prominent polycrystalline peaks observed at 2θ of 28.11°, 32.49°, 46.46°, 55.05°, 57.67°, 67.66°, 74.58° and 76.90°, which respectively correspond to (2 1 0), (2 0 1), (0 4 0), (0 3 2), (4 1 1), (5 1 0), (0 5 2), and (1 3 3) reflections of orthorhombic structure of Ag₂Se (JCPDS card No: 89–2591). The result is in agreement with the earlier reports on Ag₂Se obtained using AgNO₃ as precursor. However, purer and more intense crystalline peaks present in the nanoparticles obtained using AgCl precursor than using AgNO₃ [7–9].

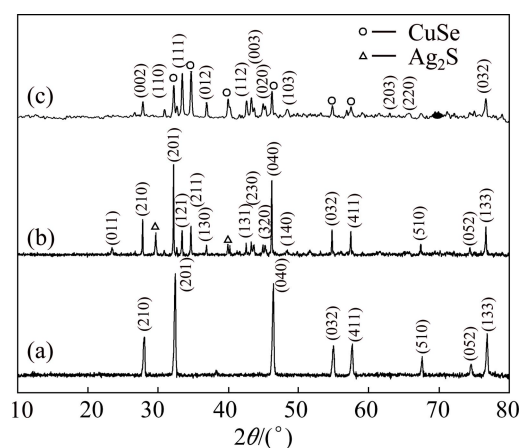


Fig. 1 XRD patterns of β -Ag₂Se (a, b) nanoparticles produced at 0.5 mol/L AgCl + 1 mol/L SeO₂ + 0.25 mol/L Na₂SO₃ (a), 1 mol/L AgCl + 2 mol/L SeO₂ + 1 mol/L Na₂SO₃ (b) and β -AgCuSe nanoparticles (c)

Figure 1(b) shows the XRD pattern of β -Ag₂Se nanoparticles obtained at 1 mol/L AgCl, 2 mol/L SeO₂ and 1 mol/L Na₂SO₃. The intensity of orthorhombic characteristic peaks gets increased in comparison with Fig. 1(a) and slightly moved towards the lower diffraction angles 2θ of 27.81°, 32.66°, 46.20°, 54.78°, 57.45°, 67.42°, 74.42° and 76.69°. This suggests that the Ag and Se ions occupy their lattice points perfectly without any defect. Subsequently, the diffraction planes show sharper and intenser signals in comparison with lower raw material concentrations. Some new orthorhombic crystalline peaks also emerge at 2θ of 23.44°, 33.42°, 34.67°, 36.91°, 42.55°, 43.27°, 44.94°, 48.45°. Although, the formation of Ag₂S impurity

observed at 2θ of 29.66° and 39.94° cannot be avoided when increasing the molar concentrations of the raw materials.

A possible mechanism for the growth of the Ag_2Se nanostructures is as follows. It is usually believed that the growth of nanostructures in solution involves two important processes, namely nucleation followed by growth. The fresh Ag_2Se nuclei are thermodynamically unstable due to their high surface energy and tend to aggregate, driven by the minimization of interfacial energy [7].

Figure 1(c) shows the XRD pattern of $\beta\text{-AgCuSe}$ nanoparticles obtained at 0.25 mol/L CuSO_4 , 0.5 mol/L AgCl , 1 mol/L SeO_2 and 0.25 mol/L Na_2SO_3 . It can be seen from the pattern that the polycrystalline peaks detected at 2θ of 27.84° , 30.90° , 33.43° , 36.99° , 42.60° , 43.32° , 43.71° , 44.97° , 48.45° , 51.69° , 75.03° and 76.74° belong to (0 0 2), (1 1 0), (1 1 1), (0 1 2), (1 1 2), (0 0 3), (2 0 0), (0 2 0), (1 0 3), (2 1 1), (1 3 1) and (0 3 2) reflections of orthorhombic structure of $\beta\text{-AgCuSe}$ nanoparticles (JCPDS card No: 25–1180), respectively. The intensity of the peaks is low and 2θ is relatively different in comparison with that of Ag_2Se ; however, the inclusion of copper ions into the Ag_2Se system has not changed its orthorhombic phase. It is noticed that the obtained results well match with the earlier report by ALIYEV [16]. It is noticed that the majority of the $\beta\text{-AgCuSe}$ crystalline peaks get broadened compared with those of $\beta\text{-Ag}_2\text{Se}$. It is presumably because Ag^+ ion is replaced by Cu^+ ion in its lattice point or occupies interstitial position in the Ag_2Se lattice. The formation of impurity could not be avoided. CuSe impurity was observed at 2θ of 32.25° , 41.97° , 45.24° , 46.24° , 54.83° , 56.86° , 60.40° and 70.44° (JCPDS No. 89–7391). XRD results confirm that the structural characteristics of $\beta\text{-Ag}_2\text{Se}$ and $\beta\text{-AgCuSe}$ nanoparticles are much better than those obtained using AgNO_3 precursor.

Lattice parameters a , b , and c values were calculated for the synthesized Ag_2Se and AgCuSe nanoparticles using “UNIT CELL Software” and their results are reported in Table 1. It is an important notice that the lattice parameters a , b and c are compressed at higher raw material concentrations in comparison with the lower concentration.

The crystallite sizes of $\beta\text{-Ag}_2\text{Se}$ and $\beta\text{-AgCuSe}$ were calculated using Debye–Scherrer formula $D=k\lambda/(\beta\cos\theta)$, where D is the crystallite size (nm), λ is the wavelength of the characteristics X-ray (\AA), θ is the Bragg diffraction angle of the respective diffraction peak ($^\circ$), β is the full width at half maximum of the peak ($^\circ$) and k is constant (0.94). The calculated crystallite sizes are given in Table 2, indicating that the crystallite size of Ag_2Se decreases with increasing the concentration of raw materials. This is contrary to the earlier report on Ag_2Se thin films where the crystallite size increases with increasing the raw material concentration [3]. Whereas, the crystallite size of $\beta\text{-AgCuSe}$ is larger than that of $\beta\text{-Ag}_2\text{Se}$ due to the inclusion of Cu^+ ions into the Ag_2Se system.

When AgCl is dissolved in ammonia, it favors to form a silver amide complex. Similarly, solutions of SeO_2 and Na_2SO_3 yield Se^{2-} and SO_3^- ions in water. In the composite solution, the presence of ions reduces silver amide complex and generates Ag^+ ions which combine with Se^{2-} ions to give insoluble Ag_2Se precipitates. The formation of Ag_2Se and AgCuSe can be understood from the following equations:

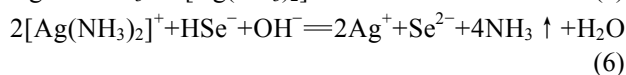
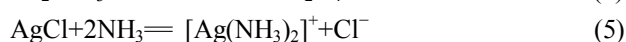
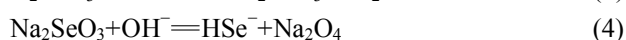
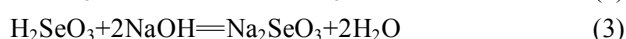
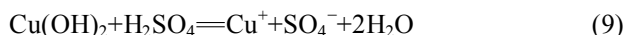
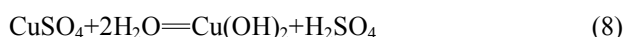


Table 1 Lattice parameters of $\beta\text{-Ag}_2\text{Se}$ and $\beta\text{-AgCuSe}$ nanoparticles

Sample	Lattice constant/ \AA								
	Observed			JCPDS			Reported		
	a	b	c	a	b	c	a	b	c
$\beta\text{-Ag}_2\text{Se}$ (0.5 mol/L AgCl + 1 mol/L SeO_2 + 0.25 mol/L Na_2SO_3)	7.140	7.825	4.290	7.050	7.850	4.330	4.333 [7]	7.062 [7]	7.764 [7]
$\beta\text{-Ag}_2\text{Se}$ (1 mol/L AgCl + 2 mol/L SeO_2 + 1 mol/L Na_2SO_3)	7.124	7.752	4.140	7.050	7.850	4.330	4.333 [3]	7.062 [3]	7.764 [3]
$\beta\text{-AgCuSe}$ (0.25 mol/L CuSO_4 + 0.5 mol/L AgCl + 1 mol/L SeO_2 + 0.25 mol/L Na_2SO_3)	4.105	4.070	6.310	4.105	4.070	6.310			

Table 2 Crystallite sizes of $\beta\text{-Ag}_2\text{Se}$ and $\beta\text{-AgCuSe}$ nanoparticles

Sample	Crystallite size/nm	
	Observed	Reported in Ref. [3]
$\beta\text{-Ag}_2\text{Se}$ (0.5 mol/L AgCl + 1 mol/L SeO_2 + 0.25 mol/L Na_2SO_3)	40	63
$\beta\text{-Ag}_2\text{Se}$ (1 mol/L AgCl + 2 mol/L SeO_2 + 1 mol/L Na_2SO_3)	30	75
$\beta\text{-AgCuSe}$ (0.25 mol/L CuSO_4 + 0.5 mol/L AgCl + 1 mol/L SeO_2 + 0.25 mol/L Na_2SO_3)	56	



Cu^+ ion replaces Ag^+ ion to form AgCuSe nanoparticles:



3.2 FTIR analysis

The spontaneous orientation of dipole moments in semiconductors is carried out by infrared spectroscopy, which gives information on atomic arrangement and inter-atomic forces in the crystal lattice itself. The FTIR vibrational bands of $\beta\text{-Ag}_2\text{Se}$ (0.5 mol/L AgCl + 1 mol/L SeO_2 + 0.25 mol/L Na_2SO_3) and $\beta\text{-AgCuSe}$ are shown in Fig. 2.

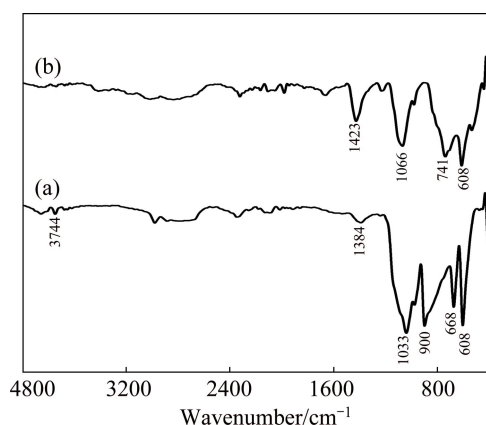


Fig. 2 FTIR spectra of $\beta\text{-Ag}_2\text{Se}$ (0.5 mol/L AgCl + 1 mol/L SeO_2 + 0.25 mol/L Na_2SO_3) (a) and $\beta\text{-AgCuSe}$ (b) nanoparticles

It can be seen from Fig. 2(a) that a band observed at 3744 cm^{-1} due to free —OH group and a band at 1384 cm^{-1} correspond to the stretching vibrations of Ag—Se bond, which confirms the formation of Ag_2Se [3]. A strong band centered at 1033 cm^{-1} is due to stretching vibration of S=O and a medium sharp peak appears at 900 cm^{-1} due to the symmetrical stretching vibration of Se—O—Se molecules. Sharp peaks are observed at 668 and 608 cm^{-1} due to the double degeneration of anti-symmetrical stretching vibration of Se—O—Se molecules and SO_4^{2-} vibration respectively, [17].

By comparing the FTIR spectra in Fig. 2(b) with Fig. 2(a), the stretching vibration of Ag—Se gets shifted to a higher frequency region (from 1384 to 1423 cm^{-1}) in comparison with Ag_2Se due to the inclusion of Cu^+ ions. Similarly, the stretching vibration of S=O gets strong and sharp at 1066 cm^{-1} , while the intensity of SO_4^{2-} vibration gets reduced at 608 cm^{-1} [17]. It is important to notice that, Cu—H bending vibration is observed at 741 cm^{-1} which is not identified in the Ag_2Se spectrum. This observation confirms the presence of copper in the Ag—Se system.

3.3 UV–Vis analysis

Figure 3 shows the optical absorption spectra of the synthesized $\beta\text{-Ag}_2\text{Se}$ (0.5 mol/L AgCl + 1 mol/L SeO_2 + 0.25 mol/L Na_2SO_3) and $\beta\text{-AgCuSe}$ nanoparticles. It is observed that the optical absorption increases from 800 nm and reaches the maximum around 250 nm . Both samples show good absorption in the visible region. However, the $\beta\text{-Ag}_2\text{Se}$ exhibited higher absorption than $\beta\text{-AgCuSe}$ nanoparticles. The optical band gap is determined by plotting a curve $(ah\nu)^2$ versus photon energy $h\nu$ and extrapolating the linear portion to the X -axis.

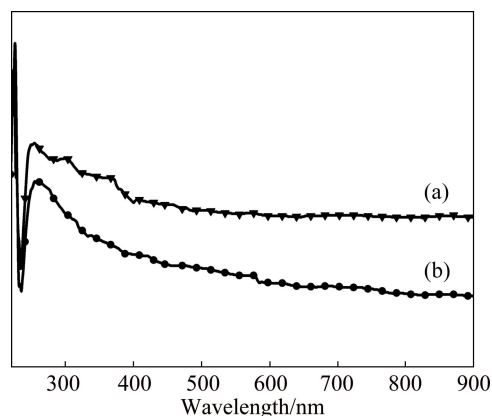


Fig. 3 Optical absorption spectra of $\beta\text{-Ag}_2\text{Se}$ (0.5 mol/L AgCl + 1 mol/L SeO_2 + 0.25 mol/L Na_2SO_3) (a) and $\beta\text{-AgCuSe}$ (b) nanoparticles

Figures 4(a) and (b) show the band gap plots for $\beta\text{-Ag}_2\text{Se}$ (0.5 mol/L AgCl + 1 mol/L SeO_2 + 0.25 mol/L Na_2SO_3) and $\beta\text{-AgCuSe}$, respectively. The band gap energy is found to be 1.78 eV for $\beta\text{-Ag}_2\text{Se}$ and 1.70 eV for $\beta\text{-AgCuSe}$. By comparing the E_g values, they are slightly higher than those of the earlier report on Ag_2Se synthesized via the solvothermal route by CAO et al [7]. They obtained E_g about 1.64 eV and their absorption peak shifted towards higher wavelength. The higher value of the band gap energy is most probably due to size quantization effects that lead to a series of discrete states in the conduction and valence bands, resulting in the increase of the effective band gap [5]. Higher absorbance in the UV–Vis region of $\beta\text{-Ag}_2\text{Se}$ evidenced for its good optical property and lower energy band gap value of $\beta\text{-AgCuSe}$ evidenced for its good conducting property.

3.4 SEM analysis

The SEM images (Fig. 5) of the $\beta\text{-Ag}_2\text{Se}$ nanoparticles (lower mole concentration of raw materials) show polyhedral- and pebble-like morphologies. Similar morphological features were recorded for $\beta\text{-Ag}_2\text{Se}$ nanocrystals synthesized via solvothermal method [11]. The mono-dispersed particles are inhomogeneously distributed on the surface.

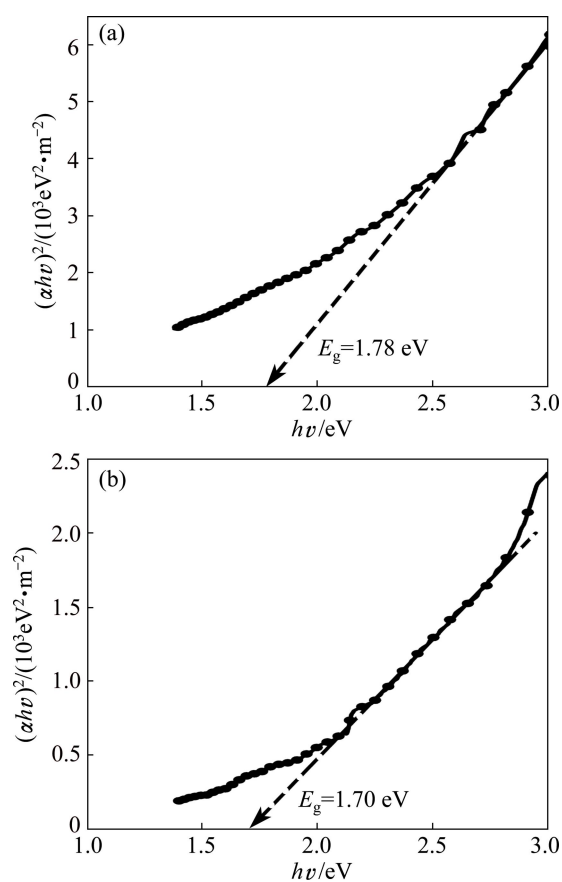


Fig. 4 $(\alpha hv)^2$ vs hv plots of β - Ag_2Se (a) and β - AgCuSe (b) nanoparticles

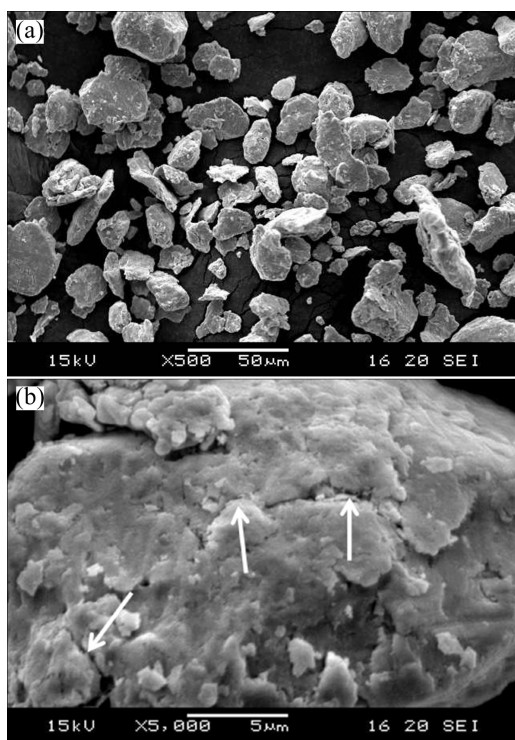


Fig. 5 SEM images of β - Ag_2Se (0.5 mol/L AgCl + 1 mol/L SeO_2 + 0.25 mol/L Na_2SO_3) nanoparticles at different magnifications

In higher magnification, β - Ag_2Se shows massive solid product, which indicates that Ag and Se bound strongly. It is observed that some cracks appear on the surface of the solid particle. It may be formed during sample preparation for SEM analysis. The average grain size was measured to be less than 10 μm .

Figure 6 shows the randomly distributed grain clusters (lower magnification) which may have formed from the aggregation of smaller nanospheres of different sizes. Due to the incorporation of Cu^+ ions in the Ag–Se system the pebble-like morphology distorted into clusters of β - AgCuSe nanospheres. The individual polygonal shape particle is obviously visible in higher magnification and the average size of the particles was found to be less than 0.5 μm .

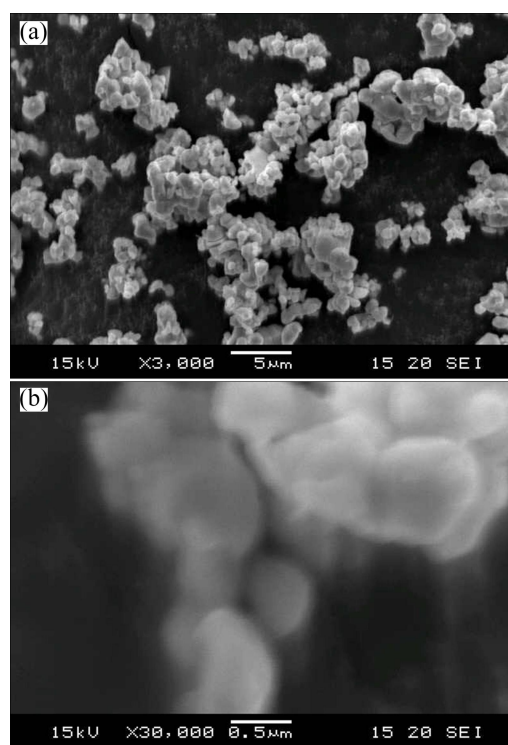


Fig. 6 SEM images of β - AgCuSe nanoparticles at different magnifications

4 Conclusions

β - Ag_2Se and β - AgCuSe nanoparticles were synthesized by simple and low cost precipitation method using AgCl as precursor. The XRD analysis confirmed the orthorhombic structure for both Ag_2Se and AgCuSe nanoparticles. It is revealed from the XRD pattern that the additional impurities were observed when the concentrations of raw materials increased. The FTIR analysis confirmed the vibrations of products Ag–Se at 1384 cm^{-1} and Cu–H at 741 cm^{-1} . The band gap energies of β - Ag_2Se and β - AgCuSe were found to be 1.78 eV and 1.70 eV, respectively. Taking into account

these values, β -Ag₂Se and β -AgCuSe seem to be much more promising materials for the semiconducting and super ionic applications, respectively. The SEM images indicate polyhedral- and pebble-like morphologies. The average grain sizes were less than 10 μ m and 0.5 μ m for β -Ag₂Se and β -AgCuSe nanoparticles, respectively. By comparing the UV–Vis spectra of β -Ag₂Se, the band gap energy was found to be lower for β -AgCuSe. Hence, it is concluded that AgCl is a simple novel precursor and can be used as an alternate precursor for AgNO₃ in the preparation of β -Ag₂Se and β -AgCuSe nanoparticles.

Acknowledgments

The authors are thankful to the DST-FIST, UGC-SAP, New Delhi, India, for providing the financial support to the Department of Physics, Manonmaniam Sundaranar University, Tirunelveli, Tamil Nadu, India and to the Professor and Head, Department of Physics, Annamalai University, India, for providing the facility of SEM analysis.

References

- [1] SANTHOSH KUMAR M C, PRADEEP B. Electrical properties of silver selenide thin films prepared by reactive evaporation [J]. Bull Mater Sci, 2002, 25: 407–411.
- [2] SOMOGYI K, SAFRAN G. Concentration dependences at the critical temperatures in vacuum topotaxial Ag₂Se thin layers [J]. Vacuum, 2005, 80: 350–355.
- [3] CHOUGALE U M, HAN S H, RATH M C, FULARI V J. Synthesis, characterization and surface deformation study of nanocrystalline Ag₂Se thin films [J]. Materials Physics and Mechanics, 2013, 17: 47–58.
- [4] CHEN Rui-zhi, XU Dong-sheng, GUO Guo-lin, GUI Lin-lin. Preparation of Ag₂Se and Ag₂Se_{1-x}Te_x nanowires by electrodeposition from DMSO baths [J]. Electrochemistry Communications, 2003, 5: 579–583.
- [5] BILJANA P, METODIJA N, IVAN GROZDANOV, SANDWIP K D. Chemical bath deposition of nanocrystalline (111) textured Ag₂Se thin films [J]. Materials Letters, 2000, 43: 269–273.
- [6] PANDIARAMAN M, SOUNDARAJAN N, VIJAYAN C, KUMAR C, GANESAN R. Spectroscopic studies on silver selenide thin films [J]. Journal of Ovonic Research, 2010, 6: 285–295.
- [7] CAO Hua-qiang, XIAO Yu-jiang, LU Yue-xiang, YIN Jie-fu, LI Bao-jun, WU Shui-sheng, WU Xiao-ming. Ag₂Se Complex nanostructures with photocatalytic activity and superhydrophobicity [J]. Nano Res, 2010, 12(3): 863–873.
- [8] LI Kun-wei, LIU Xi, WANG Hao, YAN Hui. Rapid synthesis of Ag₂Se nanocrystals by sonochemical reaction [J]. Materials Letters, 2006, 60: 3038–3040.
- [9] JAFARI M, SALAVATI NIASARI M, MOHANDS F. Synthesis and characterization of silver selenide nanoparticles via a facile sonochemical route starting from a novel inorganic precursor [J]. Journal of Inorganic and Organometallic Polymer and Materials, 2013, 23: 357–364.
- [10] LI B, XIE Y, HUANG J, QIAN Y. Sonochemical synthesis of silver, copper and lead selenides [J]. Ultrasonics Sonochemistry, 1999, 6: 217–220.
- [11] CUI Yong, CHEN Gang, REN Jin, SHAO Ming-wang, XIE Yi, QIAN Yi-tai. Solvothermal syntheses of β -Ag₂Se crystals with novel morphologies [J]. Journal of Solid State Chemistry, 2003, 172: 17–21.
- [12] BHASKER CHANDRA M, MALAR P, THOMAS O, MURTHY B S, SHIKHA V, KASIVISWANATHAN S. Characterization of silver selenide thin films grown on Cr-covered Si substrates [J]. Surf Interface Anal, 2009, 41: 170–178.
- [13] ZHANG You-jin, HU Bio, ZHANG Zu-de, QIAN Yi-tai. Room temperature redox reaction to prepare AgCuSe ternary nanorods [J]. Chinese Journal of Chemical Physics, 2005, 18: 594–598. (in Chinese)
- [14] BASKER K, SHIMOYAMA T, HOSAKA D, XIANGLIAN, SAKUMA T, ARAI M. Diffuse scattering of the superionic phase of CuAgSe [J]. Journal of Thermal Analysis and Calorimetry, 2005, 81: 507–510.
- [15] TROTS D M, SKOMOROKHOV A N, KNAPP M, FUESS H. High-temperature behavior of average structure and vibrational density of states in the ternary superionic compound AgCuSe [J]. The European Physical Journal B, 2006, 51: 507–512.
- [16] ALIYEV Y I. Structural phase transitions in AgCu_{0.5}Te_{0.5} crystals [C]//Proceedings of the National Academy of Sciences of Azerbaijan. Ankara: Gazi University Press, 2006.
- [17] BARBARA S. Infrared spectroscopy: Fundamentals and applications [M]. New Jersey: Wiley, 2004.

简单沉淀法制备 β -Ag₂Se 和 β -AgCuSe 纳米颗粒及其表征

P. PRATHIBA JEYA HELAN¹, K. MOHANRAJ¹, G. SIVAKUMAR²

1. Department of Physics, Manonmaniam Sundaranar University, Tirunelveli 627 012, India;

2. CISL, Department of Physics, Annamalai University, Annamalinagar, Tamil Nadu-608 002, India

摘要: 用 AgCl 前驱体替代传统 AgNO₃, 通过简单沉淀法合成 β -Ag₂Se 和 β -AgCuSe 纳米颗粒。结果表明: 所得 β -Ag₂Se 和 β -AgCuSe 纳米颗粒均为斜方晶系结构。随着前驱体 AgCl 浓度的增加, 出现 Ag₂S 杂质。此外, 产物的显微组织观察结果表明, 其形状为多面体和卵石状。 β -Ag₂Se 纳米颗粒因晶粒尺寸较小而具有较高的带隙能量。采用 AgCl 前驱体能成功制备纯纳米颗粒。因此, 此研究对合成 β -Ag₂Se 和 β -AgCuSe 纳米颗粒具有应用前景的前驱体是十分有意义的。

关键词: β -Ag₂Se; β -AgCuSe; 纳米颗粒; AgCl 前驱体; 沉淀法